

First-principles electronic structure study of Sc-IIA. Ormeci,^{1,*} K. Koepernik,^{1,2} and H. Rosner¹¹Max-Planck-Institut für Chemische Physik fester Stoffe, Nöthnitzer Str. 40, 01187 Dresden, Germany²Leibniz-Institut für Festkörper & Werkstofforschung (IFW) Dresden, P.O. Box 270016, 01171 Dresden, Germany

(Received 22 June 2006; revised manuscript received 11 August 2006; published 29 September 2006)

Sc crystallizes in the hcp structure at ambient pressure. The structure of the high-pressure phase Sc-II has been debated for a long time. Most recently, two different solutions for the Sc-II phase were proposed, both involving a composite incommensurate structure consisting of a host and a guest substructure. To explore the Sc-II crystal structure we perform first-principles total-energy calculations and find that the approximant modeling of the structure suggested by McMahon *et al.* [Phys. Rev. B **73**, 134102 (2006)] is the stable structure for pressures above the calculated transition pressure of 20 GPa. This theoretical value is in perfect agreement with the experimentally measured value of 23 GPa. Analyses of the band structures provide an explanation why the structure proposed by Fujihisa *et al.* [Phys. Rev. B **72**, 132103 (2005)] is not the correct Sc-II structure.

DOI: [10.1103/PhysRevB.74.104119](https://doi.org/10.1103/PhysRevB.74.104119)

PACS number(s): 61.44.Fw, 61.50.Ks, 71.15.Nc, 71.20.-b

I. INTRODUCTION

Major improvements in high-pressure experimental techniques have resulted in many high-pressure phases of elemental solids being successfully solved.^{1,2} While at ambient pressure most elements exhibit simple high-symmetry structures, some of the high-pressure phases were found to have quite complex structures with incommensurate host-guest substructures. Until lately, such structures have been observed in main-group elements only.^{1,2} Therefore, recent claims^{3,4} regarding the observation of a similar incommensurate host-guest structure in Sc, the first element of the 3d series, make Sc an interesting case from the electronic structure point of view.

Furthermore, a more recent important development concerning Sc is the observation of superconductivity with T_c values up to 8 K in the incommensurate phase.⁵ The onset of superconductivity in Sc was found by Wittig *et al.*⁶ in 1979, but without any structural characterization of the sample under high pressure. They reported a Sc-I \rightarrow Sc-II phase transition at ~ 17 GPa and an increase of T_c from 0.05 K at 18.6 GPa to 0.35 K at 21 GPa. In the work of Hamlin and Schilling, for pressures between 50 and 75 GPa, the T_c is found to increase linearly from about 4 K to ~ 8 K. Naturally, an accurate electronic structure study of Sc at increased pressures is an essential precursor to understanding the high-pressure superconductivity in the incommensurate phase of Sc.

At ambient pressure Sc crystallizes in the hexagonal closed-packed (hcp) structure.⁷ The phase that follows hcp is designated as the Sc-II phase, with a crystal structure that has remained uncertain to date.⁸ Akahama *et al.* recently studied the structural phase transitions of Sc up to pressures of 297 GPa.⁹ They found structural transitions at 23, 104, 140, and 240 GPa. The transition at 23 GPa corresponds to the transition from hcp to Sc-II. This Sc-II modification is claimed to have an incommensurate crystal structure, but two different experimental groups have reported different solutions for it.^{3,4}

Fujihisa *et al.* have proposed that the structure of Sc-II contains incommensurate host (an eight-atom framework

structure) and guest (a two-atom chain structure) substructures, both having a body-centered-tetragonal lattice.³ This proposed arrangement with superspace group symmetry $I'4/mcm(00\gamma)$, where $\gamma=1.508$ at 23 GPa, is identical to the structures of Bi-III and Sb-II.^{10,11} However, in the solution of Fujihisa *et al.*, the interatomic distance along the chains turns out to be quite short; at 23 GPa, it is 2.285 Å, about 18% shorter than the average nearest-neighbor distance in the host structure. In comparison, the corresponding differences in Bi-III and Sb-II do not exceed 2%. McMahon *et al.*, on the other hand, have claimed that an incommensurate composite structure consisting of a body-centered-tetragonal host structure and a C-face-centered guest structure provides a better overall fit to the diffraction data with reasonable guest-guest distances along the chains.⁴ According to this solution, whose superspace group is $I4/mcm(00\gamma)$ with $\gamma=1.2804$, the nearest-neighbor distance along the chains is 2.686 Å at 23 GPa, only $\sim 4\%$ shorter than the average host-host distance of 2.799 Å.

We performed first-principles, all-electron, full-potential electronic structure calculations in order to study the structural transition in Sc, from the hcp phase to the Sc-II phase. We considered the following structures: hcp, fcc, and two approximants corresponding to the above-mentioned proposals for the Sc-II modification. According to our total-energy calculations the hcp structure is favored at ambient pressures and the approximant modeling of the structure proposed by McMahon *et al.* becomes the stable structure at a transition pressure of 20 GPa, all in perfect agreement with the experimental findings of McMahon *et al.*⁴

II. COMPUTATIONAL METHOD

We used version 6.00 of the full-potential local-orbital (FPLO) band-structure method.¹² Relativistic effects were incorporated at a scalar-relativistic level. The local density approximation¹³ (LDA) to the density functional theory¹⁴ was employed through the Perdew-Wang¹⁵ parametrization of the exchange-correlation functional. We used a single numerical basis function for each of the Sc core states

($1s2s2p$). The basis set for the valence sector contained two $4s$, two $3d$, and one $4p$ radial function. The semicore states ($3s3p$) have been treated as valence states with a single numerical radial function per nl subshell. The shapes of the basis functions have been optimized, yielding a sufficient accuracy for the total energy over the range of geometries considered in this work.

The \mathbf{k} integrals are performed via the tetrahedron method with irreducible meshes corresponding to 1728 (fcc, hcp, and the approximant for the proposal of Fujihisa *et al.*) and 216 (the approximant for the proposal of McMahon *et al.*) points in the full Brillouin zone. It has been checked that the obtained per atom total energies have converged at a level of 10–100 μ hartree for all structures considered. This level of convergence is sufficient with respect to the relevant energy scale of about 1 mhartree.

III. RESULTS AND DISCUSSION

The solution for the Sc-II modification suggested by Fujihisa *et al.* is based on two body-centered-tetragonal substructures having the same a lattice parameter but with different values for the c lattice parameters. The ratio $\gamma \equiv c_H/c_G$, where c_H (c_G) is the c lattice parameter of the host (guest) substructure, is found to be an irrational number causing incommensurability along the c axis. The host substructure can be described by the Wyckoff position $8h:(x, x+1/2, 0)$ in space group $I4/mcm$, No. 140. The guest pattern is also given in the same space group with position $2a:(0, 0, 0)$. In their work McMahon *et al.* first used this model of Fujihisa *et al.* to fit their own diffraction data, taken at 23 GPa, and obtained an R factor of 1.4% with the following structural parameters: $a=7.5679$ Å, $c_H=3.4390$ Å, $c_G=2.288$ Å, $\gamma=1.5028$, and $x=0.1476$. Then, in order to avoid the occurrence of very short guest-guest distances, they searched for alternative models. By keeping the host substructure the same, but using a C -face-centered-tetragonal lattice for the guest network, they were able to lower the R factor to 1.1%. In this solution the two guest atoms in the guest substructure are positioned at $(0, 0, 0)$ and $(1/2, 1/2, 0)$. The structural parameters obtained are $a=7.5672$ Å, $c_H=3.4398$ Å, $c_G=2.686$ Å, the incommensurability ratio $\gamma=1.2804$, and $x=0.1490$.

Since both of these proposed structures contain incommensurate substructures, they have to be approximated by commensurate models with conventional three-dimensional translational symmetry in order to use standard calculational schemes for the electronic structure calculations. Regarding the solution suggested by Fujihisa *et al.* a commensurate structure formed according to $\gamma=1.50$ is used. Structural data as provided in Ref. 4 are taken as reference. The resulting approximant, referred to as $A2 \times 3$, set in space group $P4/nnc$ (No. 126), contains 16 host and 6 guest atoms in the unit cell [Fig. 1(a)]. The approximant used for modeling the solution of McMahon *et al.* has a γ value of 1.25 and contains 32 host plus 10 guest atoms [space group $P4/nbm$, No. 125, Fig. 1(b)]. It will be referred to as $A4 \times 5$.

In all noncubic structures the c/a ratios are optimized at every volume. It turns out that for hcp and for the $A4 \times 5$

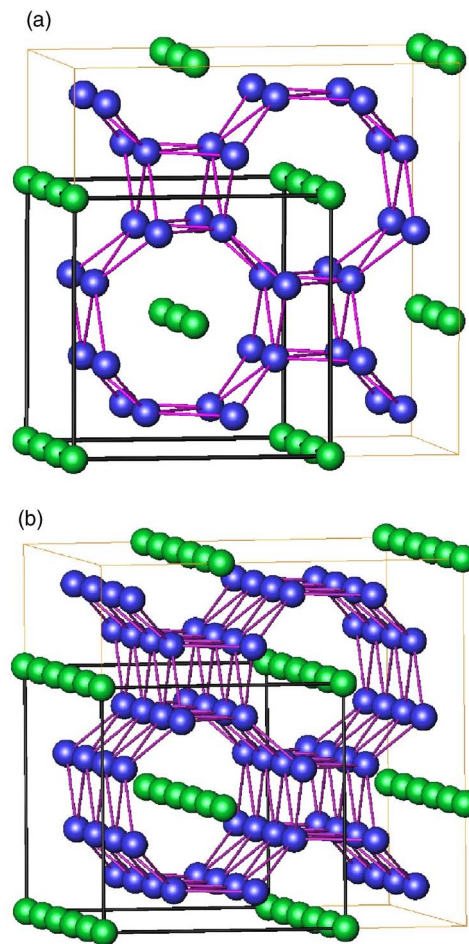


FIG. 1. (Color online) Structure of the (a) 2×3 and (b) 4×5 approximants for the crystal structure of Sc-II. The unit cells are indicated by thick black lines. Nearest neighbors in the host framework are joined by light lines.

approximant c/a is rather constant down to 70% of the experimental volume. For smaller volumes it starts to increase (by a factor of 1.14 at 40% of the volume for both structures). For the $A2 \times 3$ approximant the c/a ratio has a minimum around 70% of the volume with a value reduced by 5% compared to the value at experimental volume. Upon further decreasing the volume down to 40% it increases by a factor of 1.10.

The results of the total-energy calculations carried out for hcp, fcc, approximant $A2 \times 3$, and approximant $A4 \times 5$ are presented in Fig. 2. The hcp structure is obtained as the lowest total-energy structure for volumes between V_0 and $\approx 0.72V_0$, where V_0 is the experimental volume, 24.97 Å³ per atom.⁷ Below $0.72V_0=18$ Å³/atom, the approximant $A4 \times 5$ becomes the lowest-total-energy structure. The approximant for the Fujihisa model, $A2 \times 3$, is seen to have the highest total energy for the whole range of volumes of interest (around $V/V_0 \leq 0.58$ hcp becomes the highest-energy structure). We also observe that fcc is never stabilized, which is already known experimentally, but it is a close contender in the region of Sc-II phase with energies only less than 10 meV/atom higher than the approximant for the model of McMahon *et al.*, $A4 \times 5$.

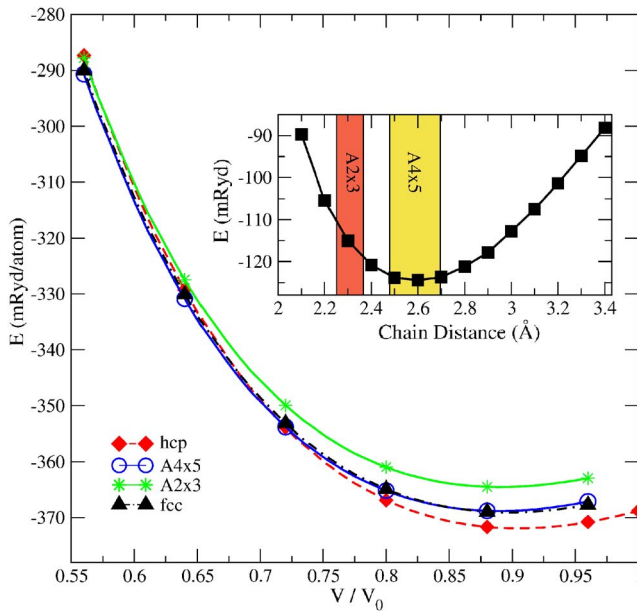


FIG. 2. (Color online) Cohesive energies of all structures considered as a function of volume. V_0 is the experimental volume per atom, 24.97 \AA^3 (Ref. 7). Lines connecting the symbols are based on the Birch-Murnaghan equation-of-state fits. Inset: Cohesive energy vs chain distance for isolated linear monatomic Sc chains.

For each model the calculated (energy, volume) data are fitted by Birch-Murnaghan-type equations of state.¹⁶ These equations of state provide pressures through $p = -\partial E(V)/\partial V$ so that enthalpies $H(p) = E(V(p)) + pV(p)$ can be calculated. The resulting volume-pressure curve for pressures up to 55 GPa is shown in Fig. 3. The hcp is found to be stable at low pressures, up to 19.7 GPa; at higher pressures, the approximant $A4 \times 5$ is the stable structure. Hence, the transition pressure between hcp and $A4 \times 5$ is 19.7 GPa, and the volume decrease at the transition pressure given by $\Delta V/V_{th}$ is 1.3%. Here, V_{th} is the theoretical equilibrium volume, $\approx 22.6 \text{ \AA}^3$ per atom, where p is zero. These results are in perfect agreement with their experimental counterparts, 23 GPa and 1.3% for the transition pressure and volume decrease, respectively.⁴ The theoretical equilibrium volume is

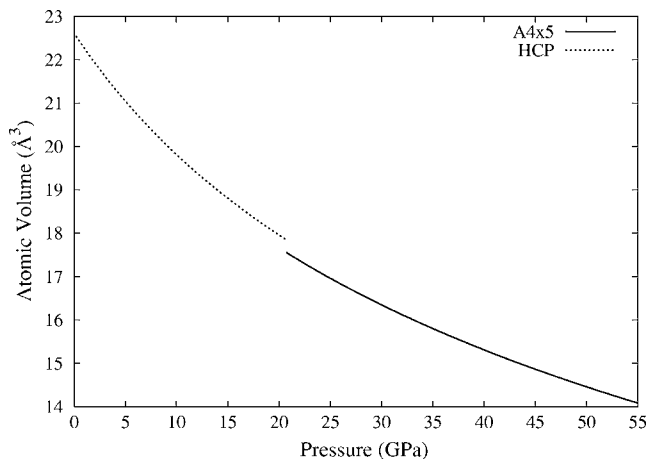


FIG. 3. The calculated equation of state for Sc up to 55 GPa.

about 9.5% smaller than the experimental volume; this is just within the typical LDA error range of 10%. However, since this overbinding effect is more or less the same in all structures considered, relative values such as volume decrease can still be obtained in good agreement with experiment.

Band structure analysis, as will be discussed in more detail below, shows that in both approximants the bands due to chain atoms have a pronounced one-dimensional (1D) character, especially in the $A2 \times 3$ structure. This suggests that host-chain interactions in Sc-II are relatively weak (although not negligible), in contrast to the situation found in Sb-II.¹⁷ In the incommensurate phase of Sb-II chemical bonding analysis based on the electron localization function revealed the existence of chemical bonds between the chain and host atoms. The weaker coupling of the chain atoms to the host framework in the case of Sc and the fact that the chains in the two approximants have very different chain distances prompt a separate study of the effects of chain distance on the energetics. Because chain-chain distances in both approximants are very large (larger than 4.87 \AA), we can safely neglect the interchain interactions. Hence, we performed total-energy calculations for isolated linear monatomic Sc chains (tetragonal space group $P4/mmm$, No. 123; the inter-chain distance $a = 8 \text{ \AA}$ is sufficient for total energy to converge, tested up to 15 \AA , and c is varied between 2.1 and 3.4 \AA). The cohesive energy versus in-chain distance, c lattice parameter, variation is shown in the inset of Fig. 2. The ranges of guest-guest distances in each approximant for atomic volumes 14– 18 \AA^3 are indicated in the figure, as well. It is clear that the “chains” of the approximant $A4 \times 5$ have lower energies than those of the approximant $A2 \times 3$. The guest-guest spacings along the linear chains of $A2 \times 3$ fall in the energetically unfavored region (on the “repulsive” arm of the energy-distance curve), whereas the chains of the $A4 \times 5$ structure have chain distances mainly in the lowest-energy region of the energy-distance curve.

The stability of the approximant $A4 \times 5$ over the $A2 \times 3$ variant can be explained in part by using the chain energy differences mentioned above. A thorough understanding requires that in addition to the effects due to different chain distances, contributions of the host-host and host-chain interactions to the cohesive energy be taken into account, as well. However, such analyses based on different decompositions of the cohesive energy are in general not very illuminating because the host-chain interactions cannot be calculated directly in a reliable way. An attempt to separate host and guest contributions by neglecting the host-guest interactions failed. So we will not pursue this line of approach here.

In Figs. 4(a) and 4(b) we show guest- and host-atom projected density of states (DOS) curves computed for the approximants $A2 \times 3$ and $A4 \times 5$, respectively, with structural parameters based on the experimental data at 23 GPa. For comparison the fcc total DOS is provided in panel (c). In the inset, the total DOS of the hcp structure at ambient pressure is shown, as well. The low-energy parts of the band extending towards $\sim -5 \text{ eV}$ are formed by the free-electron-like $4s$ states both at ambient and increased pressure. The shape of the DOS in this region remains unaffected by the applied pressure, although at 23 GPa the bottom of the band moves downward by a small amount ($\sim 0.2 \text{ eV}$), with respect to the

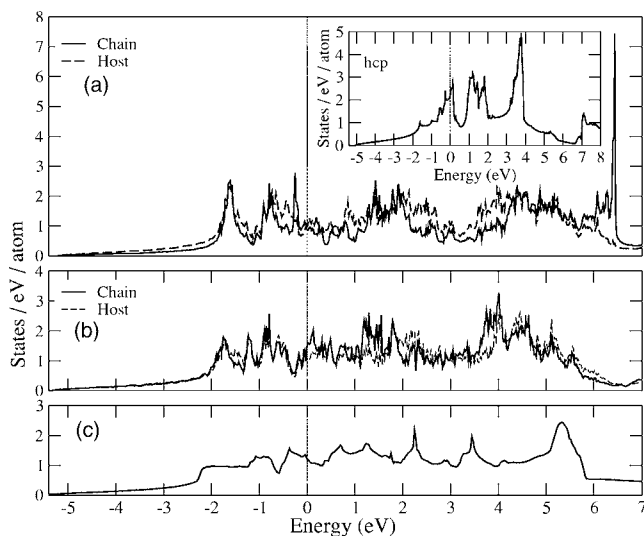


FIG. 4. Partial density of states for the guest and host atoms of Sc-II calculated by using the structural parameters based on the 23 GPa experimental data for (a) approximant $A2 \times 3$ and (b) approximant $A4 \times 5$. (c) Total density of states for the fcc structure corresponding to the same atomic volume. In the inset, total density of states for the hcp structure at ambient pressure is shown.

Fermi-level position. The approximants have many sharp peaks, mainly due to the large number of atoms in their unit cells. One notices that for the $A4 \times 5$ structure, Fig. 4(b), almost all of the sharp peaks due to chain atoms are seen to coincide with similarly sharp host peaks, whereas in the case of $A2 \times 3$, the chain peaks at ~ -0.25 and ~ 6.5 eV rising above the smoother host curve can easily be identified. This suggests that the 1D features stemming from the chain atoms are more pronounced in the approximant $A2 \times 3$ than in $A4 \times 5$.

The analyses of the atom and orbital projected band structures (fatbands) provide additional support for this suggestion. The bands with significant $3d_{3z^2-r^2}$ contributions from a chain atom are shown in Figs. 5(a) and 5(b) for $A2 \times 3$ and $A4 \times 5$ structures, respectively. The chains run along the z axis. The existence of flat, dispersionless bands in the basal plane in both figures clearly reflects the one dimensionality of the chain-atom-derived bands. The dispersions of the bands along the Γ -Z symmetry line are much larger in $A2 \times 3$ than in $A4 \times 5$. In the former the dispersions are between 1.5 and 2.2 eV, whereas in the latter the maximum dispersion is about 0.8 eV. The sharp peak in Fig. 4(a) at about -0.25 eV comes from the chain atom $3d_{3z^2-r^2}$ orbitals. The other peak at 6.5 eV is due to chain atom $3d_{xz}$ and $3d_{yz}$ orbitals (not shown).

The band structure and DOS analyses are in agreement with total-energy calculations with regards to the following picture: (1) in both approximants the guest atoms interact relatively weakly with the host atoms and thus give rise to 1D features more clearly seen in fatbands; (2) the 1D character of the bands and DOS is more pronounced in the $A2 \times 3$ approximant, implying weaker host-chain interactions in this structure than in the $A4 \times 5$ approximant; (3) due to the short guest-guest distances, the chains in the $A2 \times 3$ structure contribute less binding energy compared to the chains in the

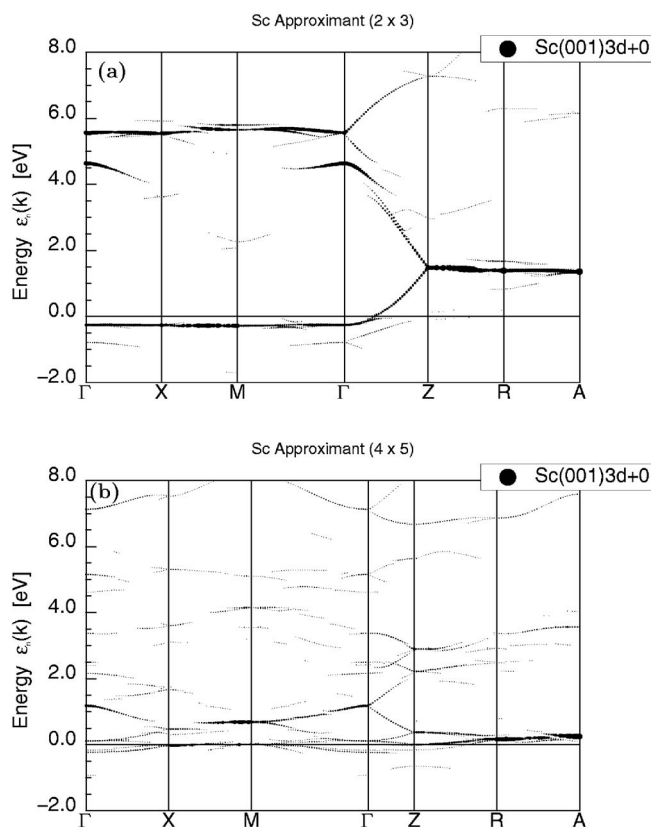


FIG. 5. Bands of (a) the approximant $A2 \times 3$ and (b) the approximant $A4 \times 5$, to which the $3d_{3z^2-r^2}$ orbital of a guest atom contributes. The size of the circle displayed in the legend corresponds to 100% contribution by the indicated orbital.

$A4 \times 5$ structure; (4) the approximant $A4 \times 5$ has lower total energies because both the guest-guest and guest-host interactions contribute more to its cohesive energy.

As is well known, when an elemental solid is subjected to increasing pressures the electronic configuration of its atoms can change dramatically. In the case of Sc, for the volumes considered here, the s - d transitions are modest. At ambient pressure, in the hcp structure the nl -projected charges are 0.70, 0.59, and 1.70 for $4s$, $4p$, and $3d$ channels, respectively. In the Sc-II phase region, for example, at V equal to two-thirds of the ambient pressure experimental volume, in the calculation for the approximant $A4 \times 5$ these numbers become 0.54–0.65, 0.27–0.51, and 1.92–2.05, respectively. Due to presence of different Wyckoff positions for guest and host atoms, the nl -projected charges (for all guest and host atoms) vary in the ranges indicated above. Since Akahama *et al.* provide a solution for the structure of Sc-V at a volume corresponding to about one-third of the ambient pressure volume (at 240 GPa),⁹ we performed a calculation at this volume using the reported structural parameters and found the following values for the nl -projected charges: 0.18, 0.03, and 2.80, respectively. Therefore, a complete $s \rightarrow d$ transfer seems to require pressures more than 240 GPa. It should also be noted that there are no significant differences between the host and guest atoms regarding the nl -projected charges in either approximant, save for some small spread of values over ranges similar to those indicated above.

In summary, the close agreement between the first-principles total-energy calculations and the experimental analyses gives unequivocal support to the solution of McMahon *et al.* as the *correct* structure of the Sc-II phase. The solution of Fujihisa *et al.*³ suffers from its anomalously short guest-guest distances because (i) these distances are mainly on the repulsive branch of the energy-chain distance curve and (ii) chain atoms interact with each other so strongly that

host-chain interactions are weaker than the corresponding situation in the structure proposed by McMahon *et al.*⁴

ACKNOWLEDGMENTS

We are thankful to M. McMahon for fruitful discussions. The DFG Emmy Noether program is acknowledged for financial support.

*Electronic address: ormeci@cpfs.mpg.de

¹U. Schwarz, Z. Kristallogr. **219**, 376 (2004).

²M. McMahon and R. Nelmes, Z. Kristallogr. **219**, 742 (2004).

³H. Fujihisa, Y. Akahama, H. Kawamura, Y. Gotoh, H. Yamawaki, M. Sakashita, S. Takeya, and K. Honda, Phys. Rev. B **72**, 132103 (2005).

⁴M. I. McMahon, L. F. Lundegaard, C. Hejny, S. Falconi, and R. J. Nelmes, Phys. Rev. B **73**, 134102 (2006).

⁵J. J. Hamlin and J. S. Schilling (private communication).

⁶J. Wittig, C. Probst, F. A. Schmidt, and K. A. Gschneidner, Jr., Phys. Rev. Lett. **42**, 469 (1979).

⁷J. Donahue, *The Structures of the Elements* (Wiley, New York, 1974), p. 84.

⁸Previous attempts at solving the structure of Sc-II phase can be summarized as follows: W. A. Grosshans, Y. K. Vohra, and W. B. Holzapfel, J. Magn. Magn. Mater. **29**, 282 (1982); Y. K. Vohra, W. A. Grosshans, and W. B. Holzapfel, Phys. Rev. B **25**, 6019 (1982); β -neptunium type primitive tetragonal lattice; J.

Akella, J. Xu, and G. S. Smith, Physica B & C **139B**, 285 (1986); primitive tetragonal lattice; Y. C. Zhao, F. Porsch, and W. B. Holzapfel, Phys. Rev. B **54**, 9715 (1996); body-centered cubic lattice.

⁹Y. Akahama, H. Fujihisa, and H. Kawamura, Phys. Rev. Lett. **94**, 195503 (2005).

¹⁰M. I. McMahon, O. Degtyareva, and R. J. Nelmes, Phys. Rev. Lett. **85**, 4896 (2000).

¹¹U. Schwarz, L. Akselrud, H. Rosner, Alim Ormeci, Yu. Grin, and M. Hanfland, Phys. Rev. B **67**, 214101 (2003).

¹²K. Koepernik and H. Eschrig, Phys. Rev. B **59**, 1743 (1999).

¹³W. Kohn and L. J. Sham, Phys. Rev. **140**, A1133 (1965).

¹⁴P. Hohenberg and W. Kohn, Phys. Rev. **136**, B864 (1964).

¹⁵J. P. Perdew and Y. Wang, Phys. Rev. B **45**, 13244 (1992).

¹⁶F. D. Murnaghan, Proc. Natl. Acad. Sci. U.S.A. **30**, 244 (1944); F. Birch, J. Geophys. Res. **57**, 227 (1952).

¹⁷A. Ormeci and H. Rosner, Z. Kristallogr. **219**, 370 (2004).